

**ABSTRACT** Electric fields can induce lateral reorganization of lipids in fluid bilayer membranes. The resulting concentration profiles readily are observed in planar-supported bilayers by epifluorescence microscopy. When a fluorescently labeled lipid was used to probe the field-induced separation of cardiolipin from egg-phosphatidylcholine, an enhanced sensitivity to the electric field was observed that is attributed to a critical demixing effect. A thermodynamic model of the system was used to analyze the results. The observed concentration profiles can be understood if the lipid mixture has a critical temperature equal to 75°K. The steady-state distribution of lipids under the influence of an electric field is very sensitive to demixing effects, even at temperatures well above the critical temperature for spontaneous phase separation, and this may have significant consequences for organization and structural changes in natural cell membranes.

Electric field-induced concentration gradients in lipid monolayers are enhanced substantially when the system is near a consolute critical point (1, 2). This critical demixing is a collective molecular effect that increases the sensitivity of a fluid system to field-induced reorganization. Here, we describe a method to study critical demixing in bilayer membranes by using an electric field applied tangent to the plane of a confined patch of supported lipid bilayer.

Lipid bilayers supported on silica substrates generally maintain a  $\approx 10$  Å layer of water between the membrane and the solid surface thus preserving many of the properties of free membranes (3–6). They are continuous with mobile components of both leaflets freely diffusing over the entire surface of the substrate. Barriers to this lateral diffusion, created either by manually scratching the membrane-coated surface or by the use of prepatterned substrates, can be used to isolate corrals of lipid bilayer with well defined geometry. Application of an electric field tangent to the membrane plane induces lateral reorganization of the lipids within each corral (Fig. 1) (7–10). Equilibrium concentration profiles are determined by the balance between forces acting on the molecules.

With this supported membrane configuration, we observed field-induced concentration profiles of a fluorescent probe lipid in a bilayer mixture of cardiolipin and egg-phosphatidylcholine (egg-PC) that have the characteristics expected for incipient critical demixing. In contrast, membranes comprised of dioleoyl-phosphatidylserine (DOPS) and egg-PC have been found to behave more like ideal fluids (10). Thus, it appears to be an attribute of cardiolipin that causes the collective demixing in the membranes studied below. A consequence of this is that egg-PC membranes containing cardiolipin are more sensitive to electric field-induced reorganization than those containing the same charge density of dioleoyl-phosphatidylserine. The work we describe here provides a quantitative

means of determining critical temperatures for demixing in bilayers even when phase separation is not observed. It is hoped that this will help to correlate the phase behavior of lipid monolayers and bilayers and to facilitate an understanding of the effects of electric fields, whether externally applied or a consequence of electrophysiology, on biological membranes.

**Thermodynamic Model with Critical Demixing.** A thermodynamic model was introduced previously to describe electric field-induced concentration gradients in planar bilayer membranes (10). This model uses Flory's approximation for the entropy of mixing in ideal liquids comprised of differently sized molecules and also accounts for electrostatic interactions within the membrane. Here, we extend it to include effects of critical demixing by incorporating Flory's expression for the free energy of mixing in nonideal liquids (11):

$$\Delta G_{\text{mix}} = k_B T (N_1 \ln(\varphi_1) + N_2 \ln(\varphi_2)) + \gamma \left( \frac{A_{m1}}{A_u} N_1 + \frac{A_{m2}}{A_u} N_2 \right) \varphi_1 \varphi_2 \quad [1]$$

where  $k_B$  is the Boltzmann constant,  $T$  is the temperature, and  $N_i$  is the number of molecules of component  $i$ . The area fractions and molecular areas appropriate for a two-dimensional system are represented by  $\varphi_i$  and  $A_{mi}$ , respectively. The unit area of the lattice,  $A_u$ , is equal to the smaller of the two molecular areas. The critical demixing parameter  $\gamma$  is defined as the differential interaction energy and can be related to the critical temperature  $T_c$ , as shown below. The first term in Eq. 1 is the entropic contribution to the free energy of mixing in ideal liquids. The second term, which is here referred to as the demixing term, accounts for critical demixing and gives rise to a critical point for phase separation.

The equilibrium concentration profiles are calculated by imposing the requirement that the gradients of chemical potentials are 0. Differentiating Eq. 1 with respect to  $N_i$  gives the entropic and demixing contributions to the chemical potential. In addition, lateral pressure in the membrane ( $\Pi$ ), the electrophoretic force ( $f_i$  = force per area acting on component  $i$ ), and electrostatic interactions within the membrane contribute to the chemical potential as described (10). Chemical potentials for a binary system including the critical demixing effect are:

$$\mu_1 = \mu_1^0 + k_B T \left( \ln(\varphi_1) - \left( \frac{A_{m1} - A_{m2}}{A_{m2}} \right) \varphi_2 \right) + \frac{A_{m1}}{A_u} \gamma \varphi_2^2 + A_{m1} \Pi - A_{m1} f_1 r + z_{m1} e \Psi \quad [2]$$

$$\mu_2 = \mu_2^0 + k_B T \left( \ln(\varphi_2) + \left( \frac{A_{m1} - A_{m2}}{A_{m1}} \right) \varphi_1 \right) + \frac{A_{m2}}{A_u} \gamma \varphi_1^2 + A_{m2} \Pi - A_{m2} f_2 r + z_{m2} e \Psi \quad [3]$$

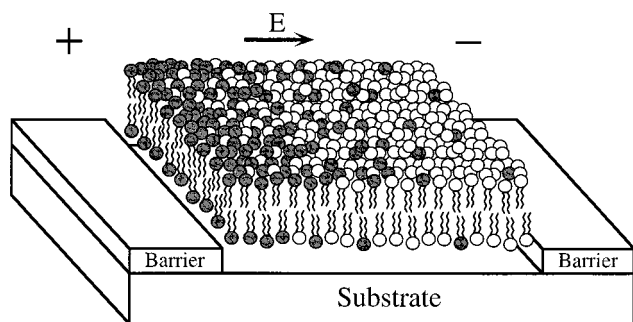


FIG. 1. Schematic diagram of an electric field-induced reorganization of lipids in a confined patch of supported bilayer membrane. A two-component system is shown in which the negatively charged lipid (shaded) builds up a concentration gradient toward the anode side of the corral. This represents an equilibrium distribution where the field-induced drift is balanced by diffusion.

where  $\mu_1^0$  and  $\mu_2^0$  are the chemical potentials of pure membranes of components 1 and 2, respectively. The molecular charge of component  $i$  is  $z_{mi}e$  where  $e$  is the elementary charge,  $\Psi$  represents the surface potential of the membrane, and  $r$  is the position along the direction of the electrophoretic field. In the following, we let  $z_{m2} = 0$  because this is a typical experimental situation. Setting the gradients of the chemical potentials to 0 and combining to eliminate the pressure terms yields

$$\left( \frac{k_B T}{A_{m1} \varphi_1} + \frac{k_B T}{A_{m2} (1 - \varphi_1)} - \frac{2\gamma}{A_u} + \frac{z_{m1} e}{A_{m1}} \frac{\partial \Psi}{\partial \varphi_1} \right) \frac{\partial \varphi_1}{\partial r} = f_1 - f_2 \quad [4]$$

with solutions given by

$$r(\varphi_1) = \frac{k_B T \ln(\varphi_1)}{A_{m1} (f_1 - f_2)} - \frac{k_B T \ln(1 - \varphi_1)}{A_{m2} (f_1 - f_2)} - \frac{2\gamma \varphi_1}{A_u (f_1 - f_2)} + \frac{z_{m1} e \Psi(\varphi_1)}{A_{m1} (f_1 - f_2)} \quad [5]$$

Eq. 5 is the inverse of the concentration profile function  $\varphi_1(r)$ . A convenient feature of this equation is that critical demixing and electrostatic effects appear as strictly additive terms.

The inverse concentration profile function can be used to relate  $\gamma$  to  $T_c$ . For any non-0 field, the gradient of the concentration profile function  $\partial \varphi_1 / \partial r$  diverges at the critical point with a corresponding 0 in the inverse expression:  $\partial r / \partial \varphi_1 = 0$ . This can be understood physically by noting that the existence of a composition gradient at equilibrium results from the balance between forward flux because of the applied field and back diffusion. At the critical point, intermolecular interactions exactly counter diffusive mixing. Thus, there is no force to oppose separation induced by the field and  $\partial \varphi_1 / \partial r$  diverges. Imposing this condition on Eq. 5 and solving for  $\gamma$ , we find

$$\gamma = \frac{k_B T_c}{2} \left( 1 + \sqrt{\frac{A_{m2}}{A_{m1}}} \right)^2 \quad [6]$$

for a binary mixture of neutral molecules. If the effective molecular area depends on composition (nonideal area of mixing),  $T_c$  also will show a pressure dependence that is not included here. Experiments in monolayers have shown that this pressure effect is relatively small in the cases studied. The relationship between  $\gamma$  and  $T_c$  is more complex for a system involving charged lipids. In general, electrostatic repulsion raises the strength of the molecular interaction energy necessary to achieve phase separation at a given temperature. For a binary system with one charged component, we find

$$\gamma = \left\{ \frac{k_B T_c}{2} \left( \frac{A_u}{A_{m1}} \left( \frac{1}{\varphi_1} \right) + \frac{A_u}{A_{m2}} \left( \frac{1}{1 - \varphi_1} \right) \right) + \frac{A_u z_{m1} e}{2 A_{m1}} \frac{\partial \Psi}{\partial \varphi_1} \right\} \Big|_{\varphi_{1crit}} \quad [7]$$

evaluated at the critical composition ( $\varphi_{1crit}$ ), which corresponds to the minimum value of the expression in curly brackets over the interval  $\{0 < \varphi_1 < 1\}$ . It turns out that  $\gamma$  is very nearly equal to  $3k_B T_c$  for a system of equally sized molecules in which one carries a net charge of  $-1$ , such as the dioleoyl-phosphatidylserine:egg-PC mixtures described (10). For a mixture with a 2:1 molecular area ratio in which the larger molecule has a charge of  $-2$ , such as cardiolipin:egg-PC,  $\gamma$  is  $\approx 2.5k_B T_c$ . This estimate of  $\gamma$  was obtained for a constant surface charge density on the supporting substrate of  $-0.25$  C/m<sup>2</sup> using the Guoy-Chapman theory to calculate  $\Psi(\varphi_1)$  (10). The relationship between  $\gamma$  and  $T_c$  is relatively insensitive to the bulk solution ionic strength.

The predicted effects of critical demixing on the concentration profile are illustrated in Fig. 2. These calculations were made for a binary system modeling cardiolipin:egg-PC with a net force on the cardiolipin of  $4 \times 10^{-16}$  newton/molecule, which is similar to experimentally realized forces. A macroscopic phase separation is predicted when the temperature is below  $T_c$ , resulting in a discontinuity in the concentration profile. It also can be seen that interactions giving rise to critical demixing have a substantial effect on the shape of the concentration profile, even at temperatures well above  $T_c$ .

A useful method for observing these concentration profiles involves probing the mixture with a small fraction ( $\approx 1\%$ ) of a fluorescently labeled lipid. The probe concentration profile can be monitored by epifluorescence microscopy and used to extract information about the distribution of the other two components. This method requires that the thermodynamic model outlined above be extended to three-component systems. The following expression for the free energy of mixing,

$$\Delta G_{mix} = k_B T \sum_i N_i \ln \varphi_i + \left( \sum_i \frac{A_{mi}}{A_u} N_i \right) \sum_{i,j} \frac{\gamma_{ij}}{2} \varphi_i \varphi_j, \quad [8]$$

can be used as a starting point to construct a model describing multicomponent systems with critical demixing. The coefficients  $\gamma_{ij}$  are symmetric with  $\gamma_{ji}$  and  $\gamma_{ii}$ , each representing the interaction energy of an  $ij$  contact relative to an  $ii$  contact. Thus,  $\gamma_{ij}$  is the critical demixing coefficient for pure binary mixture of components  $i$  and  $j$ . This expression is obtained from Eq. 1 by allowing one of the two components itself to be

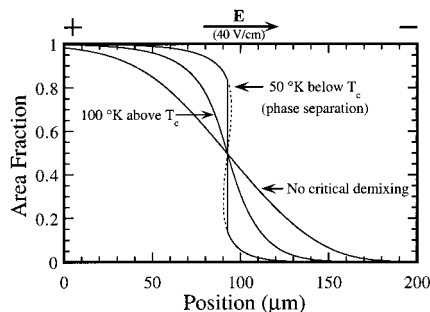


FIG. 2. Calculated equilibrium concentration profiles for a binary mixture modeling cardiolipin and egg-PC. The force acting on each cardiolipin molecule is  $4 \times 10^{-16}$  newton, which is achieved experimentally at a field strength of  $\approx 40$  V/cm. The net force is less than the Coulombic force caused by electroosmotic drag. Three curves are shown illustrating the results for different relative critical points; the ambient temperature for all calculations is 295°K. A discontinuity in the concentration profile is predicted for temperatures below  $T_c$  caused by macroscopic phase separation. Critical demixing produces a substantial effect on the concentration profile even at temperatures well above  $T_c$ .

a binary mixture and carrying out the logical expansion. A similar model has been used to describe multicomponent lipid systems at the air water interface, and it has been found to be consistent with experimental results (12). Using Eq. 8 to generate the entropic and demixing terms, we constructed a system of equations for the chemical potential gradients that is solved numerically to calculate concentration profiles. This method is used in the analysis of the cardiolipin:egg-PC mixture described below.

## RESULTS AND DISCUSSION

The fluorescently labeled lipid NBD-PE [*N*-(7-nitrobenz-2-oxa-1, 3-diazol-4-yl)-1,2-dihexadecanoyl-sn-glycero-3-phosphoethanolamine, triethylammonium salt] was used to probe the electric field-induced separation of cardiolipin and egg-PC in a confined patch of lipid bilayer. Supported membranes consisting of egg-PC, cardiolipin, and NBD-PE in a 85:7:1 mole ratio were formed by vesicle fusion and partitioned into isolated corrals by manually scratching the membrane-coated surface. Application of an electric field tangent to the membrane plane caused both the probe and the cardiolipin to drift toward the anode side of the corral and build up concentration gradients against the barrier. When the field was removed, the membranes relaxed back to uniformity by diffusive mixing. An epifluorescence image of the steady-state concentration profile of the probe is shown in Fig. 3. It took roughly 60 min at a field strength of  $\approx 40$  V/cm for this profile to reach steady-state. The lower panel in Fig. 3 contains quantitative information about the probe concentration, which was obtained from image analysis. (Calibration experiments on membranes with fixed compositions confirmed that fluorescence from the NBD-PE probe was related linearly to its concentration in the membrane up to a  $\approx 0.065$  area fraction. Probe concentrations remained well below this value in all of the experiments described here.)

The most distinctive feature of the probe concentration profile is that it reached a maximum a substantial distance from the barrier. This result appears paradoxical because both the probe and cardiolipin are expected to have roughly the same charge per area and thus should not be separated from

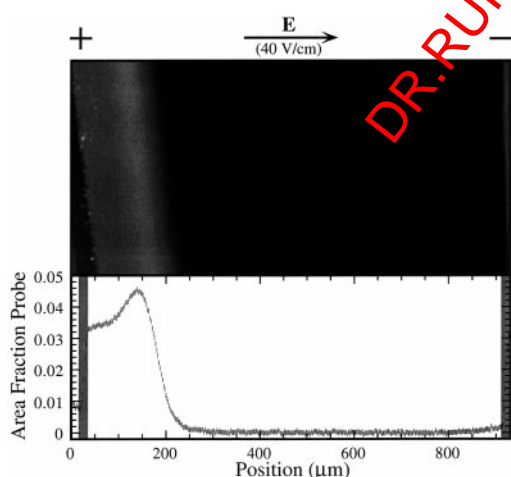


FIG. 3. Image of the steady-state concentration profile of NBD-PE in a mixture of cardiolipin and egg-PC taken with a Zeiss Axiovert 100 epifluorescence microscope equipped with a Princeton Instruments (Trenton, NJ) model TK512D back-illuminated charge-coupled device camera. This distribution was created with an applied field of  $\approx 40$  V/cm in a patch of membrane confined between scratch boundaries. Image analysis was used to obtain a quantitative trace of the profile, which is shown in the lower panel. The scale on this profile was calibrated against the fluorescence intensity from the uniform membrane (1% area fraction) before application of the field.

each other solely by action of an electric field. We suggest that the peak in the probe concentration profile was caused by collective demixing between cardiolipin and the other components in the membrane. Preferential association of cardiolipin molecules with themselves should tend to exclude the probe from regions of high cardiolipin concentration. Alternatively, if cardiolipin actually occupies significantly less area in the membrane than two NBD-PE molecules, a peak in the probe distribution can result from the difference in charge density. This is essentially a buoyancy effect whereby the molecular species with a higher charge density sinks to the lower energy position in the electrophoretic potential gradient, causing the less dense species to float on top. As discussed

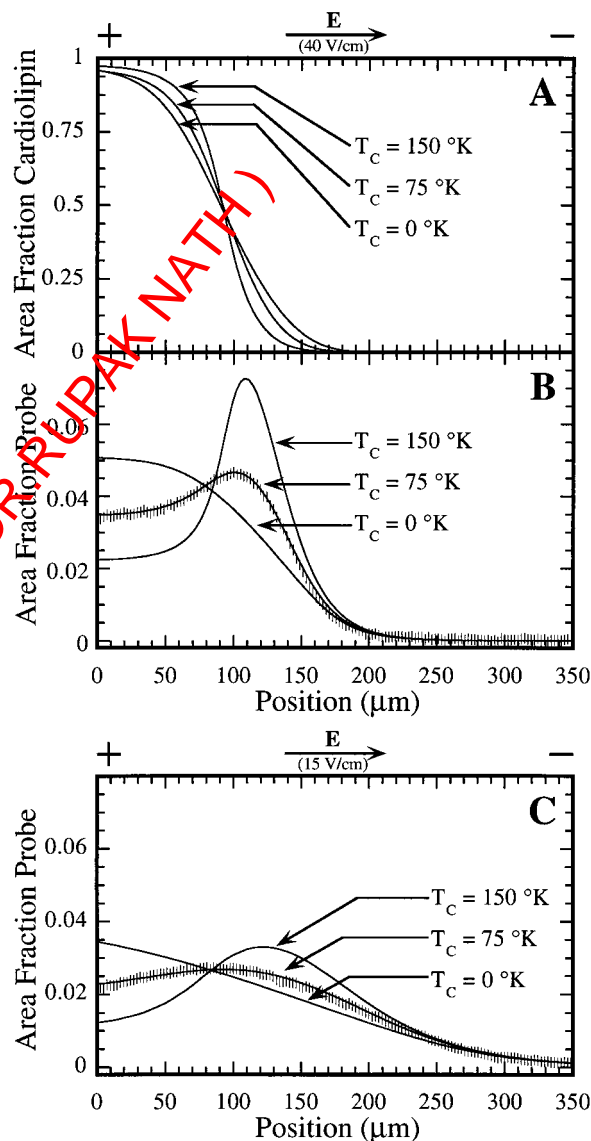


FIG. 4. Comparison of measured concentration profiles (vertical bars) with calculations (continuous lines) for different degrees of critical demixing. The ambient temperature in all calculations and experiments was 295°K. (A) Cardiolipin concentration profiles in the three-component mixture described in the text with a net force of  $4 \times 10^{-16}$  newton/molecule on the cardiolipin corresponding to a field strength of  $\approx 40$  V/cm. (B) Probe concentration profiles in the same mixture. The net force acting on the probe was taken to be  $2 \times 10^{-16}$  newton/molecule. An overlay of the experimentally measured profile closely matches the calculated curve for a critical temperature of 75°K. (C) Calculated probe concentration profiles and experimental data for the same mixture at a field strength of  $\approx 15$  V/cm. Again, the best fit was obtained for a critical temperature of 75°K.

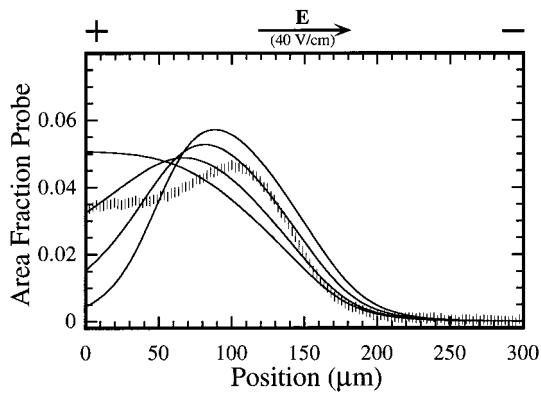


FIG. 5. Calculated concentration profiles (continuous lines) for different molecular area ratios of cardiolipin to NBD-PE compared with the observed profile (vertical bars). The membrane was treated as an ideal liquid at 295°K with a force of  $4 \times 10^{-16}$  newton/molecule on the cardiolipin and  $2 \times 10^{-16}$  newton/molecule on the NBD-PE. A monotonic profile (top curve at 0 position) is predicted if cardiolipin occupies twice the area of NBD-PE. At lower size ratios (1.67:1, 1.33:1, and 1:1), progressively larger peaks in the calculated concentration profiles arise from the buoyancy effect. These have a different characteristic shape than peaks caused by demixing (see Fig. 4).

below, demixing and buoyancy produced characteristically different signatures on the functional form of the concentration profile, which suggests that the peak we observe was primarily caused by demixing.

Comparisons of the measured profiles with calculations for different degrees of demixing are presented in Fig. 4. The curves in Fig. 4 *A* and *B* were generated using a force of  $4 \times 10^{-16}$  newton/molecule on the cardiolipin (molecular charge of  $-2$ ) and half that on the NBD-PE (molecular charge of  $-1$ ). These forces are consistent with the applied field strength of  $\approx 40$  V/cm along with the usual amount of electroosmotic drag (7, 13, 14). Direct measurements of the probe drift velocity in these membranes,  $\approx 0.47$   $\mu\text{m/s}$ , provide independent confirmation of this molecular force. The molecular areas of egg-PC and NBD-PE were both taken to be  $60 \text{ \AA}^2$  whereas the cardiolipin was assumed to occupy twice this area (15). Three different values of the critical demixing coefficient between cardiolipin and the other components were used and were labeled with the corresponding critical temperature. Here, the probe was assumed to mix ideally with egg-PC, which is consistent with earlier results (10). Concentration profiles of cardiolipin are shown in Fig. 4*A* with the probe concentration profile shown in Fig. 4*B*. The best fit to the experimental data corresponds to a critical temperature of 75°K for cardiolipin:egg-PC mixtures. The same critical temperature is obtained from an analysis of concentration profiles created at a field strength of  $\approx 15$  V/cm (Fig. 4*C*). This confirms that the experimentally measured concentration profile has the expected dependence on field strength for a system in which cardiolipin is being separated from the probe based on the demixing effect.

Calculated concentration profiles illustrating the separation of cardiolipin from the NBD-PE probe because of differences in charge density are presented in Fig. 5. These curves were generated using the same forces per molecule as above but allowing the effective molecular area of cardiolipin in the membrane to vary. If the cardiolipin has twice the area of the probe, the charge densities are the same, and a strictly monotonic concentration profile of the probe is predicted. At lower size ratios, the charge density of cardiolipin is higher than that of the probe, expelling it from the lowest energy positions by the buoyancy effect. No size ratio between the two molecules could be found that predicts concentration profiles consistent with observations. Although minor effects of charge density differences may be present, demixing appears to be the primary cause of the peak in the probe concentration profile.

Determination of the critical temperature for spontaneous phase separation provides a measurement of the degree to which collective demixing affects a system. Higher critical temperatures indicate stronger demixing effects and consequent increased sensitivity to perturbations such as those caused by an electric field. The methods described here allow quantitative comparison of critical demixing in membranes even when spontaneous phase separation is not observed.

We thank Steven Andrews for help writing the C program used to solve the multicomponent problem numerically. We also thank James Sabry and Jim Spudich for use of microscope imaging facilities in their lab and Rüdiger Koker for helpful discussions. This work was supported in part by the National Science Foundation Biophysics Program (to S.G.B.) and by National Science Foundation grant MCB-9310256 (to H.M.M.).

1. Lee, K. Y. C., Klingler, J. F. & McConnell, H. M. (1994) *Science* **263**, 655–658.
2. Lee, K. Y. C. & McConnell, H. M. (1995) *Biophys. J.* **68**, 1740–1751.
3. Bayerl, T. M. & Bloom, M. (1990) *Biophys. J.* **58**, 357–362.
4. Johnson, S. J., Bayerl, T. M., Mcdermott, D. C., Adam, G. W., Rennie, A. R., Thomas, R. K. & Sackmann, E. (1991) *Biophys. J.* **59**, 289–294.
5. Koenig, B. W., Krueger, S., Orts, W. J., Majkrzak, C. F., Berk, N. F., Silverton, J. V. & Gawrsh, K. (1996) *Langmuir* **12**, 1343–1350.
6. Sackmann, E. (1996) *Science* **271**, 43–48.
7. Groves, J. T. & Boxer, S. G. (1995) *Biophys. J.* **69**, 1972–1975.
8. Groves, J. T., Wülfing, C. & Boxer, S. G. (1996) *Biophys. J.* **71**, 2716–2723.
9. Groves, J. T., Ulman, N. & Boxer, S. G. (1997) *Science* **275**, 651–653.
10. Groves, J. T., Boxer, S. G. & McConnell, H. M. (1998) *Proc. Natl. Acad. Sci. USA* **95**, 13390–13395.
11. Guggenheim, E. A. (1952) *Mixtures*, eds. Fowler, R. H., Kapitza, P., Mott, N. F. & Bullard, E. C. (Oxford Univ. Press, Oxford).
12. Hagen, J. P. & McConnell, H. M. (1996) *Biochim. Biophys. Acta* **1280**, 169–172.
13. Stelzle, M., Miehlich, R. & Sackmann, E. (1992) *Biophys. J.* **63**, 1346–1354.
14. McLaughlin, S. & Poo, M.-M. (1981) *Biophys. J.* **34**, 85–93.
15. Gennis, R. B. (1989) *Biomembranes* (Springer, New York).